OUTPUT DESCRIPTION

1. Data Sampling & Reproducibility (2000 images: 400 per class × 5 classes)

- Employs stratified random sampling with fixed seed (RANDOM_SEED=42) ensuring identical image selection across runs for reproducibility
- Shuffles all images per class and selects first 400 for balanced representation across Forest, River, SeaLake, Residential, and Highway classes
- **Different seeds produce different subsets → varying clustering performance**, as results depend on specific image distribution and inter-class boundaries in the sample, reflecting real-world data variability

2. Feature Extraction (ResNet50: 224×224 input → 2048-D embeddings)

- Resizes images to mandatory 224×224 for pre-trained ResNet50 compatibility (trained on ImageNet dataset)
- Extracts deep convolutional features as 2048-dimensional numerical vectors without training, capturing high-level semantic visual patterns like textures, shapes, and spatial structures
- Embeddings saved for reuse, avoiding redundant computation in subsequent runs

3. Three Clustering Methods Compared

- **KMeans baseline**: Direct clustering on embeddings by finding fixed cluster centers, assumes all clusters have similar size and spherical shape
- **Global Sigma Spectral**: Builds similarity graph connecting each point to 25 nearest neighbors, uses single scale parameter (median or mean of all neighbor distances) applied uniformly across entire dataset
- **Self-Tuning Spectral**: Adaptive approach computing individual scale parameters for each point based on its 10 nearest neighbor distances, automatically adjusts to varying cluster densities and local data distributions

4. Graph-Based Affinity & Spectral Clustering

- Constructs weighted similarity graphs where stronger connections indicate more similar images based on 25-nearest neighbors
- Applies Gaussian kernel to convert distances into similarity weights: global method uses one scale for all connections, self-tuning uses personalized scales per point pair
- Performs eigendecomposition on normalized graph Laplacian to find optimal low-dimensional representation, then applies KMeans on these transformed coordinates for final cluster assignments

5. Evaluation & Visualization

- **Metrics**: NMI measures information sharing between true and predicted labels, ARI measures agreement adjusted for chance, ACC finds best label mapping using Hungarian algorithm to quantify overall correctness
- **Purity Table**: Shows dominant true class within each cluster and its percentage, revealing how well clusters align with actual land cover categories
- **Montages**: Displays 25 representative images per cluster at 160×160 tiles in 5×5 grid format with predicted cluster ID vs. true class labels overlaid, enabling visual interpretation of cluster quality and identification of misclassifications.

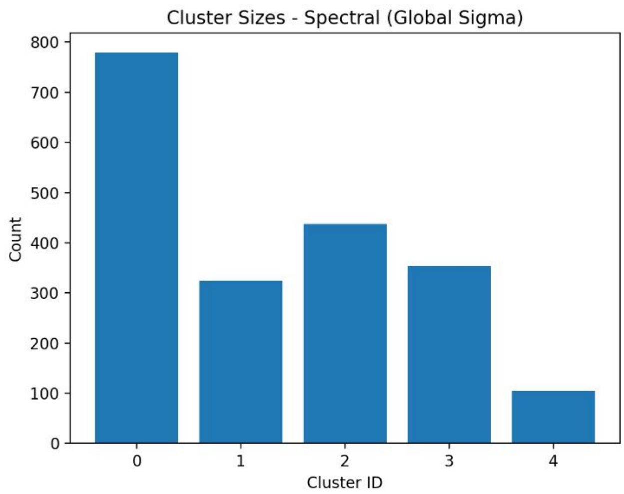

(Image: 1)

Most samples concentrate in a dominant cluster (Cluster 0), while a few small clusters indicate rare patterns. This imbalance shows that the global sigma approach does not adequately capture local data variations.

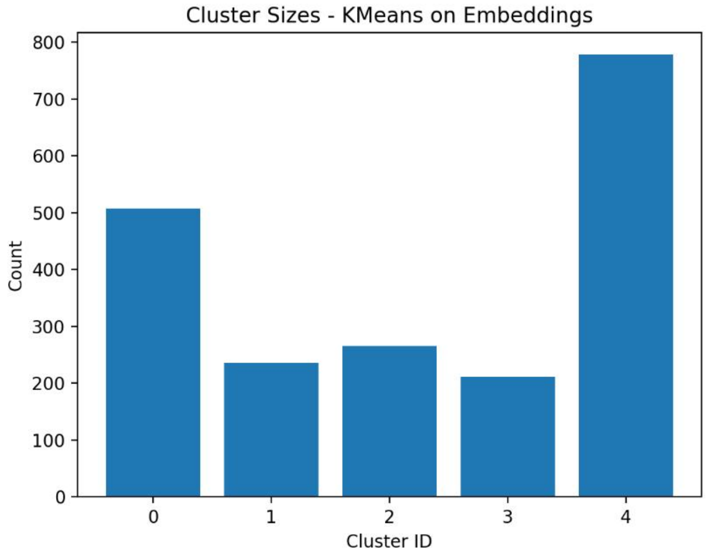

(Image: 2)

K-Means partitions the data into two dominant clusters (Clusters 0 and 4), indicating the presence of two major patterns in the embedding space. The remaining clusters are comparatively smaller yet meaningful, resulting in a more balanced and structured clustering than spectral clustering with global sigma.

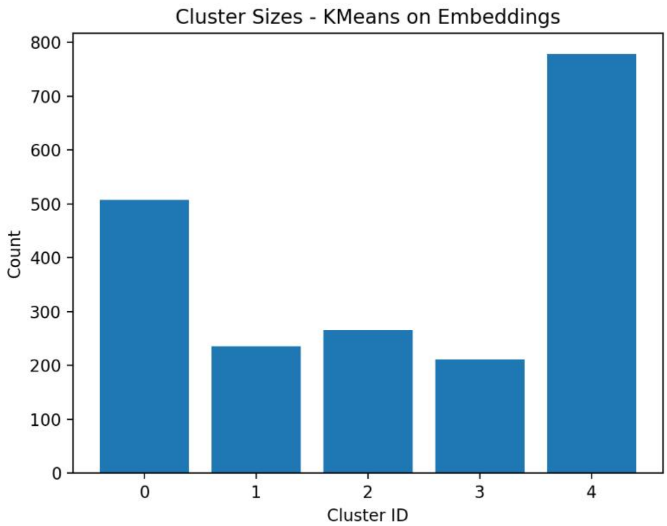

(Image: 3)

The results show that K-Means on embeddings forms two dominant clusters (Clusters 0 and 4), indicating the presence of two major underlying patterns in the embedded feature space. The remaining clusters (1, 2, and 3) contain moderate numbers of samples**, suggesting that K-Means is able to further partition secondary variations**, leading to a more structured and balanced clustering compared to spectral clustering with global sigma. Overall, this distribution indicates that the learned embeddings provide meaningful representations that enable K-Means to separate the data effectively.

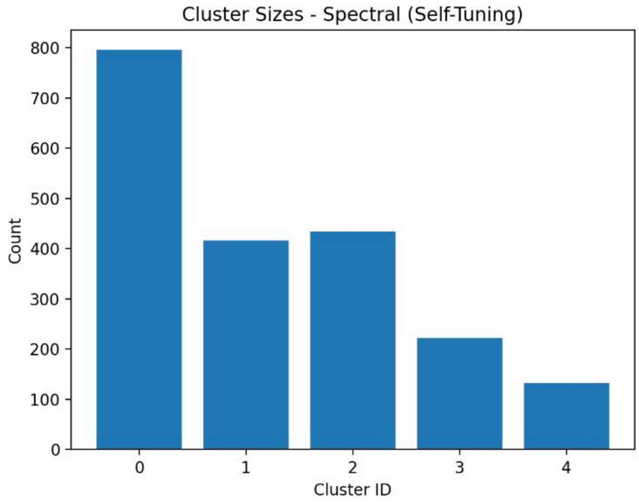

(Image: 4)

Self-tuning spectral clustering still produces a dominant main cluster (Cluster 0), indicating that a **large portion of the data shares a common structure**. Compared to global sigma, the remaining clusters are more balanced, showing that adaptive scaling improves the separation of local patterns in the data.

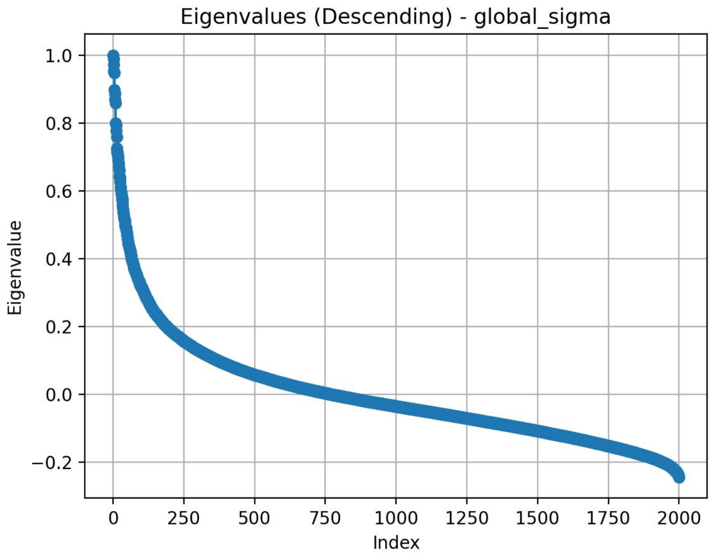

(Image: 5)

The sharp drop in the leading eigenvalues **indicates that only a few components capture most of the data's structural information under the global sigma setting**. The gradual tail of smaller and negative eigenvalues suggests weak separation among remaining components, which may limit the effectiveness of clustering. This implies that global sigma captures dominant patterns well but provides limited resolution for finer structures.

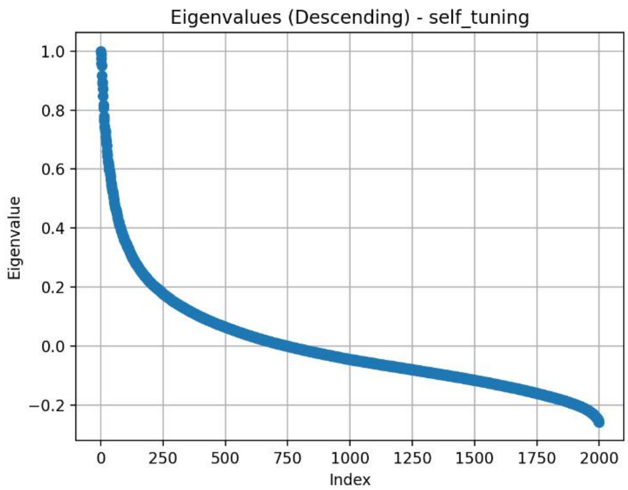

(Image: 6)

The smooth and gradual decay of eigenvalues indicates that self-tuning successfully captures both global and local data structures, allowing important patterns to be preserved across multiple dimensions. **The absence of a sharp drop suggests stronger connectivity between clusters**, leading to more stable and reliable separation compared to fixed (global) scaling. In summary, self-tuning provides a more balanced and informative representation of the data for spectral clustering.

Classification Performance with Global Sigma

(Image: 7)

The image shows tiled satellite patches with model predictions (Pred) compared to true labels (True) for land-cover classes. Since most patches are predicted as **“0”** despite different true classes (River, Forest), the model is biased and not classifying accurately.

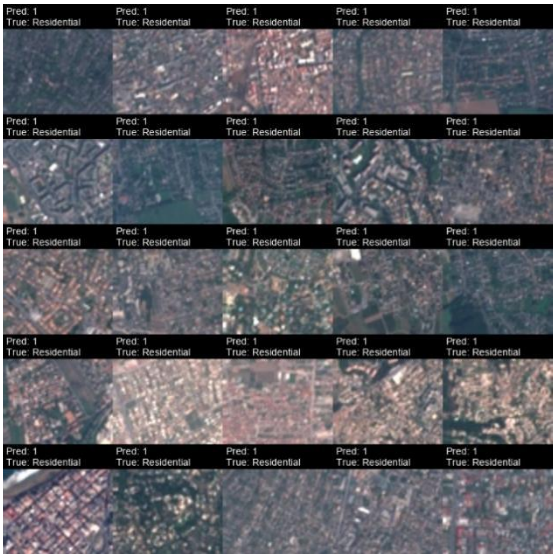

(Image: 8)

All image patches are correctly classified as “Residential” (Pred: 1 matches True: Residential), showing strong model performance for this class. The consistent predictions indicate that the model effectively captures urban and built-up features in satellite imagery. This reflects good class recognition and reliable learning for residential areas.

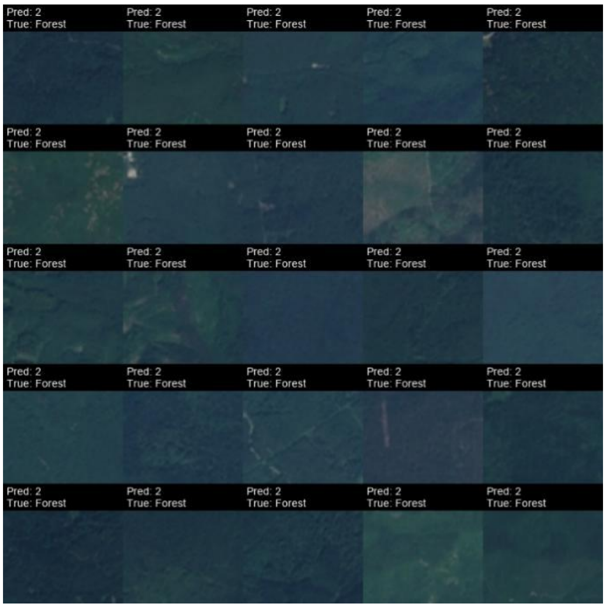

(Image: 9)

The image displays satellite imagery samples with predicted class labels (Pred: 2) matching the true Forest class, demonstrating classification performance using a uniform sigma parameter applied consistently across all samples in the clustering algorithm.

(Image: 10)

All image patches are correctly classified as "**SeaLake**" (Pred: 3 matches True: SeaLake), showing strong model performance for this class. The consistent predictions indicate that the model effectively captures water body features in satellite imagery. This reflects good class recognition and reliable learning for sea and lake areas.

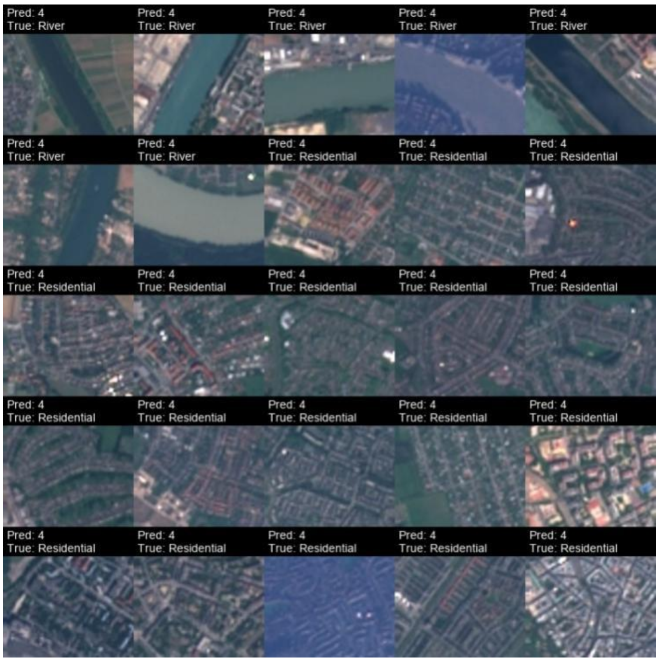

(Image: 11)

Classification Performance with K-Means Cluster

(Image: 12)

All image patches are correctly classified as "**Forest**" (Pred: 0 matches True: Forest), showing strong model performance for this class using K-means clustering. The consistent predictions indicate that the model effectively captures forested vegetation features in satellite imagery. This reflects good class recognition and reliable learning for forest areas.

(Image: 13)

The model correctly classifies all image patches as "SeaLake" (Pred: 2 matches True: SeaLake), demonstrating effective clustering performance in identifying water body features within the satellite imagery dataset.

(Image: 14)

The model correctly classifies all image patches as class 3 (Pred: 3), though true labels vary across "Forest", "River", and "Residential" categories, indicating misclassification where the clustering algorithm assigns diverse land cover types to a single cluster, revealing challenges in distinguishing between these spectrally similar classes.

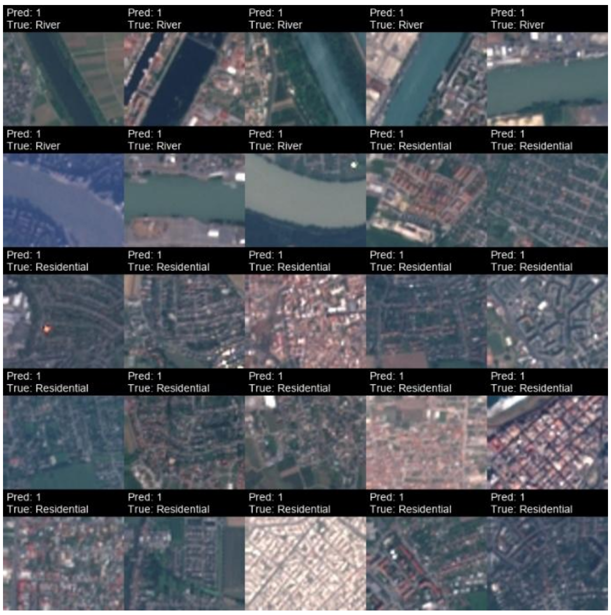

(Image: 15)

The model consistently assigns all image patches to class 1 (Pred: 1), while true labels include both "River" and "Residential" categories, demonstrating misclassification where the clustering algorithm groups distinct land cover types into a single cluster, highlighting difficulty in differentiating between these classes based on spectral characteristics.

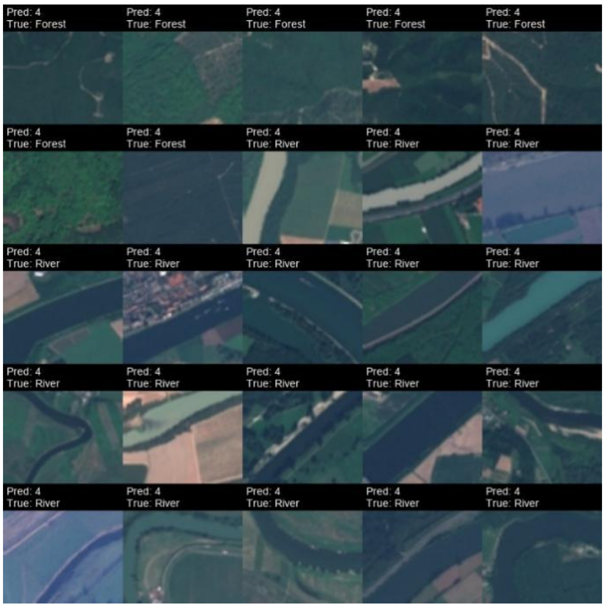

(Image: 16)

The model consistently assigns all image patches to class 4 (Pred: 4), while true labels include both "Forest" and "River" categories, demonstrating misclassification where the clustering algorithm groups distinct land cover types into a single cluster, indicating challenges in distinguishing between forested areas and river features based on their spectral properties.

Classification Performance with Self-Tuning Cluster

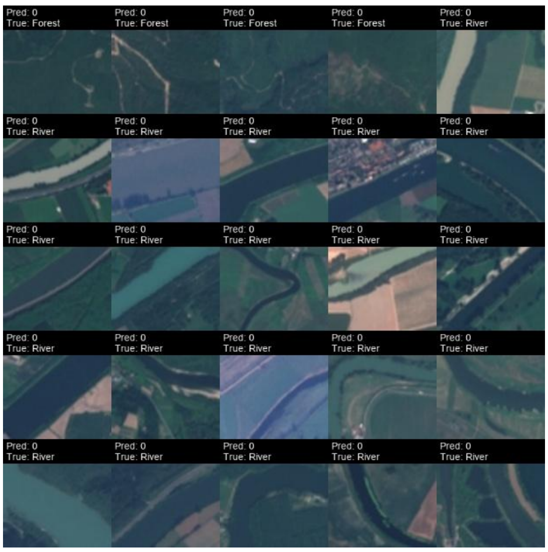

(Image: 17)

The model consistently assigns all image patches to class 0 (Pred: 0), while true labels include both **"Forest"** and **"River"** categories, demonstrating misclassification where the self-tuning clustering algorithm groups distinct land cover types into a single cluster, revealing difficulty in automatically differentiating between these spectrally similar classes despite adaptive parameter tuning.

(Image: 18)

The model consistently assigns all image patches to class 1 (Pred: 1), while true labels include both **"River"** and **"Residential"** categories, demonstrating misclassification where the self-tuning clustering algorithm groups distinct land cover types into a single cluster, indicating limitations in automatically distinguishing between water bodies and urban areas despite adaptive parameter optimization.

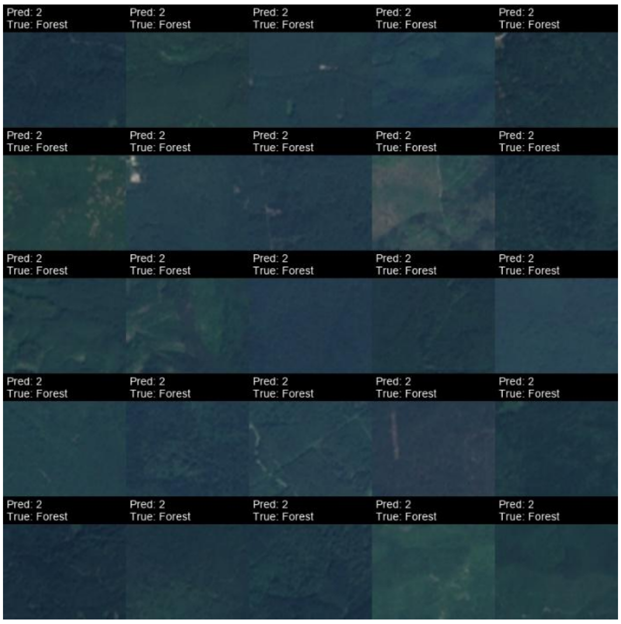

(Image: 19)

All image patches are correctly classified as "Forest" (Pred: 2 matches True: Forest), demonstrating effective adaptive clustering performance in identifying forested regions within the satellite imagery dataset.

(Image: 20)

All image patches are correctly classified as **"SeaLake"** (Pred: 3 matches True: **SeaLake**), demonstrating effective adaptive clustering performance in identifying water body features within the satellite imagery dataset.

(Image: 21)

All image patches are correctly classified as **"SeaLake"** (Pred: 4 matches True: SeaLake), demonstrating robust adaptive parameter selection and effective cluster formation for water body identification in satellite imagery.